HHS Public Access

Author manuscript

J Vis Exp. Author manuscript; available in PMC 2026 March 09.

High-Throughput Dissociation and Orthotopic Implantation of Breast Cancer Patient-Derived Xenografts

Stuart A. Clayton[1], **Alan D. Mizener**[2], **Elena Pugacheva**[2], **Emidio E. Pistilli**[1,2,3]

[1] Division of Exercise Physiology, Department of Health Professions, West Virginia University School of Medicine

[2] Cancer Institute, West Virginia University School of Medicine

[3] Department of Microbiology, Immunology, and Cell Biology, West Virginia University School of Medicine

Abstract

Patient-derived xenografts (PDXs) provide a clinically relevant method for recapitulating tumor-involved cell types and the tumor microenvironment, which is essential for advancing knowledge of breast cancer (BC). Additionally, PDX models enable the study of BC systemic effects, which is not possible using in vitro models. Traditional methods for implanting BC xenografts typically involve anesthesia and sterile surgical procedures, which are time-consuming, invasive, and limit the scalability of PDX models in BC research. This protocol describes a simple and scalable method for the orthotopic implantation of BC PDXs in mice. The immunodeficient mouse strain NOD.Cg-*Prkdc*^{scid}*Il2rg*^{tm1Wjl}/SzJ (NSG) was used for PDX engraftment. Human BC samples obtained from IRB-consented patients were mechanically and enzymatically dissociated, then resuspended in a solution of basement membrane extract (BME) and RPMI 1640. Animals were restrained by scruffing, and depilatory cream was applied to remove hair from the fat pads at the fourth inguinal nipple, followed by injection. Approximately 2 million cells in a 100 µL suspension were bilaterally injected orthotopically into the mammary fat pads using a 26 G needle. Notably, no anesthetic was required, and the total procedure time was under 5 min, from cell preparation to injection. After a growth period of several months, tumors were excised and processed for authentication. Validation included receptor status assessment using immunohistochemistry with specific antibodies for traditional BC receptors (i.e., ER, PR, HER2). Tumor morphology was confirmed with hematoxylin and eosin (H&E) staining, which was interpreted by a pathologist. Genetic similarity to the patient sample was verified through bulk RNA sequencing and short tandem repeat (STR) analysis. This approach to PDX engraftment and validation supports the rigorous development of models and high-throughput tumor implantation, enabling well-powered studies across various BC subtypes.

Corresponding Author Emidio E. Pistilli, epistilli2@hsc.wvu.edu.

A complete version of this article that includes the video component is available at http://dx.doi.org/10.3791/67607.

Disclosures

The authors declare that they have no conflicts of interest to disclose.

Introduction

Breast cancer (BC) is diagnosed in over 2 million women worldwide each year[1]. In order to advance the basic biological understanding of BC and successfully translate novel therapeutics to approved treatments, preclinical animal models that retain the defining features of patient tumors are necessary. Patient-derived xenografts (PDXs) have been demonstrated to recapitulate tumor heterogeneity with high fidelity when implanted orthotopically, including histopathology, receptor expression, and genetic aberrations[2,3,4]. Importantly, they also retain stromal cells that contribute to the microenvironment of the tumor, such as vasculature, immune cells, and cancer-associated fibroblasts. Albeit, they are gradually replaced by murine host stromal cells with passaging[5]. PDXs also enable the study of systemic complications resulting from tumor growth, such as fatigue[6,7], which is not currently possible using *in vitro* models.

Successful BC PDX engraftment does, however, require an immunodeficient mouse strain, with the most commonly used strain being NSG (NOD.Cg-*Prkdc*^{scid} *Il2rg*^{tm1Wjl}/SzJ). NSG mice are devoid of adaptive immunity and exhibit highly defective innate immunity[8]. BC PDX engraftment has been achieved in other immunodeficient strains, such as SCID/Beige (CB17.Cg-*Prkdc*^{scid}*Lyst*$^{bg\text{-}J}$/Crl), with similar engraftment rates[4].

Traditional methods of implanting BC PDXs involve surgically implanting a tumor fragment into the mammary fat pad[9], and this approach leads to successful engraftment at favorable rates. However, the need for sterile surgical procedures and anesthetic use makes it time-consuming, thus limiting the number of mice that can be implanted in a certain time window. Given PDXs' potential predictive benefits of drug responses in tumors and use in precision medicine[10], having a simple and reproducible workflow for implanting PDXs homogeneously across mice is vital. This article demonstrates the dissociation of human breast tumors into a single cell suspension and subsequent orthotopic injection into mammary fat pads of immunodeficient mice.

Protocol

This protocol adheres to the guidelines established by the West Virginia University (WVU) Institutional Animal Care and Use Committee. Female NOD.Cg-*Prkdc*^{scid}*Il2rg*^{tm1Wjl}/ SzJ (NSG) mice, aged 8 weeks or older and weighing approximately 25 g, were used for tumor cell injections. Breast cancer tumor tissue was procured at West Virginia University Cancer Institute (Morgantown, WV) and by the NCI Cooperative Human Tissue Network under approved WVU Institutional Review Board protocol and WVU Cancer Institute Protocol Review and Monitoring Committee. Informed written consent was obtained from the patients. All procedures were conducted under aseptic conditions within a Class II biological safety cabinet, following appropriate personal protective equipment (PPE) protocols. The details of the animals, reagents, and equipment used in this study are provided in the Table of Materials.

1. High-throughput enzymatic dissociation of tumor tissue

1. Thaw and combine enzymes H, R, and A from the human tumor dissociation kit in a sterile C-tube. Add 200 µL of enzyme H, 100 µL of enzyme R, and 25 µL of enzyme A. Bring the final volume to ~5 mL by adding 4.7 mL of sterile RPMI 1640 medium to the C-tube.

   NOTE: Dulbecco's Modified Eagle Medium (DMEM) can be used in place of RPMI 1640.

2. Tumor fragments can be cut and frozen as described in existing protocols[9]. Transfer thawed tumor fragments and accompanying freezing medium onto one half of a sterile 100 mm culture dish. Using sterile forceps, transfer the tumor fragments to a sterile 5 mL microtube.

   NOTE: A sterile hypodermic needle may be used as an alternative to forceps. A 35 mm dish can be used in place of a 5 mL microtube.

3. Wash the tumor fragments with 1–3 mL of sterile phosphate-buffered saline (PBS, 1x). Manipulate the fragments in the solution using forceps to ensure thorough removal of the residual freezing medium.

4. Transfer the washed fragments to a 2 mL microtube using forceps. Apply 1 mL of triple antibiotic (TAB) solution to the tumor fragments and incubate for 10 min at room temperature.

   NOTE: This step may be skipped if desired. 10x TAB stock can be made by dissolving 1% gentamicin, 1% clindamycin, and 0.5% polymyxin B sulfate in sterile 1x PBS. Dilute to 1x TAB solution in sterile 1x PBS.

5. Using ethanol-disinfected forceps or a new sterile pair, transfer the disinfected fragments to a new 5 mL microtube. Perform a second wash with 1–3 mL of sterile PBS. Transfer the washed fragments to the dry half of the 100 mm culture dish from step 1.2.

6. Using two sterile No. 10 scalpel blades, thoroughly mince the tumor tissue. Transfer the minced tumor fragments onto one blade and deposit them into the C-tube containing the prepared enzyme solution. Securely fasten the tube lid until a final click is felt.

7. Invert the C-tube several times to ensure an even distribution of tumor fragments within the enzyme solution.

8. Place the C-tube in the mechanical dissociator. Invert the tube and ensure all contents are submerged in the medium. The tube will be in an inverted position in the machine.

   1. Secure the tube in a slot with the indented part facing the operator. If applicable, place the heater around the tube.

9. Select the **37C_h_TDK_3** program from the touchscreen interface. This program operates for 60 min at 37 °C. For softer tumors, **37C_h_TDK_1** or 2 can be used.

   NOTE: For the greatest efficiency, it is recommended that the mice be prepared for injection during this dissociation period by applying depilatory cream to the injection sites.

10. Upon completion of the dissociation program, inspect the tube contents. No visible tumor fragments should remain.

    NOTE: If fragments are present, additional dissociation time may be required. In such cases, run the program for an additional 20–30 min.

11. Once adequate dissociation is achieved, centrifuge the C-tube at 200 × *g* for 5–8 min at 4 °C to pellet dissociated cells. Carefully remove the supernatant using vacuum aspiration or a pipette.

12. Resuspend the cell pellet in 5–10 mL of fresh RPMI medium. Transfer the cell suspension to a 15 mL conical tube for easier manipulation. Centrifuge the cell suspension at 200 × *g* for 5–8 min at 4 °C. Carefully aspirate the supernatant.

    NOTE: This step may be omitted if the cell pellet is small. In such cases, the cells are resuspended directly in the desired volume of media and then combined with basement membrane extract (Matrigel) to minimize cell loss.

13. Resuspend the cell pellet in a volume of RPMI 1640, equivalent to half the desired final injection volume. RPMI 1640 and Matrigel will be combined in a 1:1 v/v ratio, with a final injection volume of 100 µL per injection site.

    NOTE: For bilateral injection in 4 mice, the total required volume is 800 µL. Therefore, resuspend the cells in at least 400 µL of RPMI 1640. To account for potential volume loss, adding an additional 20% to the final volume is advisable, maintaining the 1:1 v/v ratio. Alternatively, DMEM or 1x PBS can be used in place of RPMI 1640.

14. Count the resuspended cells using a hemocytometer or automated method. Dilute as needed to achieve the desired concentration for injection. A starting point of approximately 1–2 million cells per injection site is suggested.

15. In a 2 mL round-bottom microcentrifuge tube, combine the desired amount of diluted cell suspension in RPMI with an equal volume of Matrigel. Gently mix the suspension by repeated pipetting to ensure homogeneity.

    NOTE: Following the previous step, add 400 µL of diluted cell suspension to 400 µL of Matrigel. Consider the number of injection needles to be used and factor in associated volume losses. Keep Matrigel on ice at all times. Do not thaw it until cells are resuspended, as it will solidify quickly. Recommended to maintain small aliquots (e.g., 120 µL) for quick thawing and combination in 2 mL tube.

16. Maintain the cell suspension on ice until ready for injection.

2. Orthotopic inguinal mammary fat pad injection of dissociated PDX

1. Determine the mass of each mouse using a calibrated balance. Apply a thin layer of depilatory cream to the target injection site(s). Using a sterile cotton swab, massage the cream in alternating clockwise and counterclockwise motions to facilitate rapid fur removal.

    1. Remove excess fur and depilatory cream using a sterile gauze sponge. Ensure complete hair removal at the injection area.

        NOTE: Do not exceed 60 s of depilatory cream exposure to prevent skin irritation. Mice can be shaved prior to the application of depilatory cream to further minimize exposure time. This step can be performed during tumor dissociation to optimize time efficiency and minimize the duration of cell suspension storage on ice.

2. Conduct a thorough visual inspection of each mouse to assess fitness for injection. Evaluate for any signs of pain, distress, illness, or other contraindications.

3. Using a 1 mL syringe without an attached needle, gently aspirate the cell suspension up and down to ensure homogeneity. Attach a 26 G needle to the 1 mL syringe and withdraw the desired injection volume. Eliminate any air bubbles from the syringe by gentle tapping or flicking.

    NOTE: It is recommended not to exceed 600 µL per syringe to facilitate single-handed injection.

4. Place the prepared syringe horizontally on top of the ice container, with the needle oriented away from the operator. Position the ice container and needle on the same side as the operator's dominant hand or preferred injection hand. Remove the mouse from its housing and disinfect the injection area using an alcohol cleansing pad.

5. Securely restrain the mouse by grasping the dorsal skin firmly at the nape and back. Ensure sufficient immobilization to clearly expose the mammary fat pads. The inguinal mammary fat pad spans from the nipple to the top of the hip. It can be observed as soft, pinkish tissue in the described area underneath the skin.

    NOTE: An assistant operator may use flat-sided forceps to pinch and elevate the skin containing the fat pad. This technique helps ensure that the operator performing the injection successfully targets the fat pad.

6. Place the mouse in a supine position. Insert the needle (bevel up) at a 45-degree angle, pointing toward the hip approximately 0.5–1 cm caudal to the fat pad, adjusting for needle length.

    1. Advance the needle into the fat pad. In a controlled manner, inject the desired volume of cell suspension. Efficient injection speed will help minimize animal agitation from prolonged restraint.

7. Post-injection, rotate the needle 180 degrees (bevel down). Maintain needle position briefly before slow withdrawal to minimize cell loss from the injection site. If any bleeding occurs, apply standard gauze or hemostatic gauze as necessary.

8. Repeat steps 2.6 and 2.7 for the contralateral fat pad if bilateral injections are required. For multiple animals, repeat steps 2.2–2.7 as needed.

3. Follow up procedures

1. Dispose of all sharps in designated sharps containers. Dispose of all other contents in proper waste containers.

2. If bleeding occurs during injection, monitor mice for at least 1 h afterward to ensure hemostasis.

3. Monitor body mass on a weekly basis. Assess tumor volume once growth becomes palpable.

Representative Results

This study outlines an efficient and non-surgical approach for the orthotopic implantation of patient-derived breast cancer xenografts in mice. Breast tumor tissue was dissociated using human-specific enzymes and mechanical agitation, resuspended in a 1:1 v/v ratio of Matrigel: RPMI 1640, and injected orthotopically into the inguinal mammary fat pads of NSG mice (Figure 1 and Figure 2). To ensure the fidelity of the PDX models, the concordance of the original patient tumor sample with the passaged tumors was validated with established histopathological and genomic techniques. Receptor expression was profiled using immunohistochemistry (IHC) staining of standard breast cancer receptors, including estrogen receptor (ER), progesterone receptor (PR), and human epidermal growth factor receptor 2 (HER2) (Figure 3). Cellular morphology was assessed using hematoxylin and eosin (H&E) staining of sectioned tumor slices and expert pathologist interpretation of the stained sections. Preservation of the genetic landscape and retention of human cells was validated using bulk RNA-sequencing and short tandem repeat (STR) authentication (Figure 4 and Table 1). Additionally, pathogen testing identified no contamination of the patient or passaged tumor samples, which is an essential verification step given the use of immunodeficient mice.

NSG mice were prepared for injection using a depilatory cream applied in alternating clockwise and counterclockwise motions to thoroughly remove fur from the inguinal mammary fat pad area (Figure 2A). Excess depilatory cream was wiped from exposed abdominal skin using sterile gauze, and the area was disinfected with an alcohol pad (Figure 2B). A sterile needle loaded with dissociated tumor cells was positioned at approximately a 45-degree angle 0.5–1 mm caudal to the fourth inguinal nipple mammary fat pads (Figure 2C). Tumor cells were injected in a controlled manner into the fourth inguinal nipple mammary fat pads (Figure 2D). Tumor growth was initially detected by digital palpation of the fat pads. Subsequently, tumor volume progression was quantitatively tracked using magnetic resonance imaging (MRI) (Figure 2E). Both body weight (Figure 2F) and tumor

volumes (Figure 2G) were measured weekly to monitor for fluctuations in weight and progression of tumor volumes. Tumors were visually inspected to monitor for wounds such as ulceration that would necessitate premature termination. Successful bilateral engraftment of the PDX in the inguinal mammary fat pads is shown in Figure 2H, and the fat pads following the excision of the tumors are shown in Figure 2I.

The representative PDX (PEN_056) originated from a 31-year-old Caucasian female with stage 3A invasive mammary carcinoma. The primary tumor, collected from the right breast, had a receptor status of ER and PR negative, HER2 positive (ER-PR-HER2+). IHC staining for ER, PR, and HER2 receptors showed concordance between the patient and PDX tumors (Figure 3). However, the PDX does show a greater expression of HER2, which may be due to a selective growth of HER2+ cells. Pathologist evaluation of H&E stained sections confirmed poorly differentiated carcinoma with consistent morphology and cytology in both the patient and PDX samples (Figure 3).

Short tandem repeat (STR) genotyping confirmed >80% similarity across the 13 autosomal loci defined by the American Type Cell Culture Collection (ATCC) ASN-0002-2022 consensus guidelines plus 3 additional loci (Table 1). Bulk RNA-sequencing (RNA-seq) of the patient tumor sample and PDX confirmed equivalent levels of alignment to the latest human reference genome (T2T CHM13v2.0), with 82.3% and 79.1% of reads aligning, respectively. Furthermore, the patient tumor and PDX showed a strong positive correlation with a Pearson r value of 0.9559 (Figure 4A). Gene set enrichment analysis comparing PDX vs patient tumor revealed that the top 10 significantly enriched pathways from gene ontology biological processes were predominantly immunologic gene sets, suggesting that the majority of the transcriptional variance between PDX and patient tumor derives from the lack of immune cells in the PDX sample (Figure 4B).

Discussion

This article presents an efficient, high-throughput method for orthotopically implanting BC PDXs into the inguinal mammary fat pads of immunodeficient mice. This optimized workflow enables the single researcher to implant PDXs into dozens of mice per day, supporting large-scale and adequately powered studies. The capacity to simultaneously dissociate and implant multiple unique PDXs also enables precision oncology approaches. Beyond time efficiency, the dissociation of the tumors creates a homogenous suspension of cell types that is evenly distributed between mice. In our experience, this homogeneity contributes to consistent engraftment and tumor growth rates.

While generally effective, this protocol may require modifications in certain scenarios. For instance, the standard 1 h runtime on the mechanical dissociator occasionally proves insufficient for complete tumor tissue dissociation. While firmly grasping the C-tube, flick it downward several times to accumulate any stray tissue in the bottom. If visible tissue fragments remain, continue dissociation and reinspect at 15 min intervals. It is important to note that some tissues, particularly fibrous or adipose tissue, may resist dissociation and require manual removal to prevent needle clogging during injection.

We recommend using the smallest gauge needle possible (27 G or 26 G) to minimize animal distress and reduce the risk of cell backflow from the injection site, which could impact engraftment success and tumor growth rates. However, if undissociated tissue or adipose fragments remain, a larger gauge needle (16 G or 18 G) may be necessary, albeit with increased risks of bleeding or cell loss. Regardless of the needle gauge selected, animal handling proficiency is the most important component in performing the injections effectively. No anesthesia is used in this protocol, and while this saves time, it also allows the animal to have a degree of mobility when injections are being performed. If adequate restraint is not achieved when scruffing, abrupt limb movements may cause puncture of vessels, the creation of an exit wound that prevents cell retention, or abdominal wall punctures. Sufficient practice injecting is strongly recommended prior to injecting valuable cells.

The dissociation technique described is highly transferable and can be employed in the implantation of numerous other tumor types for both orthotopic and subcutaneous models. However, at least in the context of BC, subcutaneous implantation should be avoided. Orthotopic BC PDX injection results in superior host vascularization of the engrafted tumor compared to subcutaneous, and inguinal fat pad implantation leads to greater engraftment rates than thoracic fat pad[11]. Additionally, orthotopically implanted PDXs have a shorter engraftment time and a more rapid growth rate compared to subcutaneous injections[12]. It should also be noted that while dissociation facilitates rapid tumor cell injection, it inherently results in the loss of cell-to-cell context; thus, it may not be an appropriate approach in all cases. For instances demanding authentic cell interaction (e.g., spatial transcriptomics of the tumors), injecting minced tumor pieces or implanting fragments may be preferred.

While essential for PDX studies, the use of immunodeficient mice introduces certain limitations. From a logistical perspective, a fully sterile environment, including housing, food, and water, is required. This further necessitates dedicated housing areas for immunodeficient animals to reduce the risk of infection, potentially increasing housing costs. This increased susceptibility to infections is why an antibiotic incubation step for the tumor fragments is suggested prior to dissociation. However, some studies have shown that antibiotic use in cell culture leads to alterations in gene expression profiles[13]. Given this, researchers should evaluate the use of antibiotics for each study. While the effective absence of an immune system allows PDXs to engraft, it also precludes the study of the numerous immune system effects on BC progression[14].

This method demonstrates high fidelity to the patient tumor samples. Histopathological authentication confirmed the concordance of the passaged PDX relative to the patient tumor sample, as expected. The high alignment of reads to the human genome strongly suggests that the PDX maintains a high percentage of human cells following passage. This is further supported by the >80% similarity in STR profiles and strong positive correlation in the RNA-seq data between the patient tumor and PDX. Molecular adaptations in peripheral tissues of PDX mice following breast tumor growth are also consistent with molecular adaptations in human BC patients. Bulk RNA-seq and proteomic analyses of skeletal muscles from BC PDX mice are strikingly concordant with molecular changes in muscle

biopsies obtained from patients diagnosed with early-stage BC[6,7]. Collectively, the similarity of STR profiling and RNA-seq, coupled with consistent adaptations in peripheral tissues, provides compelling data for the use of BC PDX mice in preclinical trials.

Acknowledgments

We would like to acknowledge the generous contributions of the patients who provided tumor samples for the development of PDXs. Emidio Pistilli acknowledges the significant prior contributions of Hannah Wilson, MD/PhD. This research was supported by the following organizations: National Institutes of Arthritis, Musculoskeletal and Skin Diseases (NIAMS) under award number R01AR079445 (Pistilli); the WVU Genomics Core Facility (U54GM104942); the WVU Animal Model and Imaging Facility (P20GM121322, U54GM104942, P20GM144230, P30GM103488); National Institutes of General Medical Sciences under award number P20GM121322 (Lockman). Figure 1 was created with BioRender.com.

References

1. Sung H et al. Global cancer statistics 2020: GLOBOCAN estimates of incidence and mortality worldwide for 36 cancers in 185 countries. CA Cancer J Clin. 71 (3), 209–249 (2021). [PubMed: 33538338]
2. Hidalgo M et al. Patient-derived xenograft models: an emerging platform for translational cancer research. Cancer Discov. 4 (9), 998–1013 (2014). [PubMed: 25185190]
3. DeRose YS et al. Tumor grafts derived from women with breast cancer authentically reflect tumor pathology, growth, metastasis and disease outcomes. Nat Med. 17 (11), 1514–1520 (2011). [PubMed: 22019887]
4. Zhang X et al. A renewable tissue resource of phenotypically stable, biologically and ethnically diverse, patient-derived human breast cancer xenograft models. Cancer Res. 73 (15), 4885–4897 (2013). [PubMed: 23737486]
5. Yoshida GJ Applications of patient-derived tumor xenograft models and tumor organoids. J Hematol Oncol. 13 (1), 1–16 (2020). [PubMed: 31900191]
6. Wilson HE et al. Human breast cancer xenograft model implicates peroxisome proliferator-activated receptor signaling as driver of cancer-induced muscle fatigue. Clin Cancer Res. 25 (7), 2336–2347 (2019). [PubMed: 30559167]
7. Wilson HE et al. Skeletal muscle reprogramming by breast cancer regardless of treatment history or tumor molecular subtype. NPJ Breast Cancer. 6 (1), 18 (2020). [PubMed: 32550263]
8. Shultz LD et al. Human lymphoid and myeloid cell development in NOD/LtSz-scid IL2Rγnull mice engrafted with mobilized human hemopoietic stem cells. J Immunol. 174 (10), 6477–6489 (2005). [PubMed: 15879151]
9. DeRose YS et al. Patient-derived models of human breast cancer: Protocols for in vitro and in vivo applications in tumor biology and translational medicine. Curr Protoc Pharmacol. 14, Unit14.23, (2013).
10. Whittle JR, Lewis MT, Lindeman GJ, Visvader JE Patient-derived xenograft models of breast cancer and their predictive power. Breast Cancer Res. 17 (1), 17 (2015). [PubMed: 25849559]
11. Fleming JM, Miller TC, Meyer MJ, Ginsburg E, Vonderhaar BK Local regulation of human breast xenograft models. J Cell Physiol. 224 (3), 795–806 (2010). [PubMed: 20578247]
12. Okano M et al. Orthotopic implantation achieves better engraftment and faster growth than subcutaneous implantation in breast cancer patient-derived xenografts. J Mammary Gland Biol Neoplasia. 25 (1), 27–36 (2020). [PubMed: 32109311]
13. Ryu AH, Eckalbar WL, Kreimer A, Yosef N, Ahituv N Use antibiotics in cell culture with caution: Genome-wide identification of antibiotic-induced changes in gene expression and regulation. Sci Rep. 7 (1), 7533 (2017). [PubMed: 28790348]
14. Amens JN, Bahçecioglu G, Zorlutuna P Immune system effects on breast cancer. Cell Mol Bioeng. 14 (4), 279–292 (2021). [PubMed: 34295441]

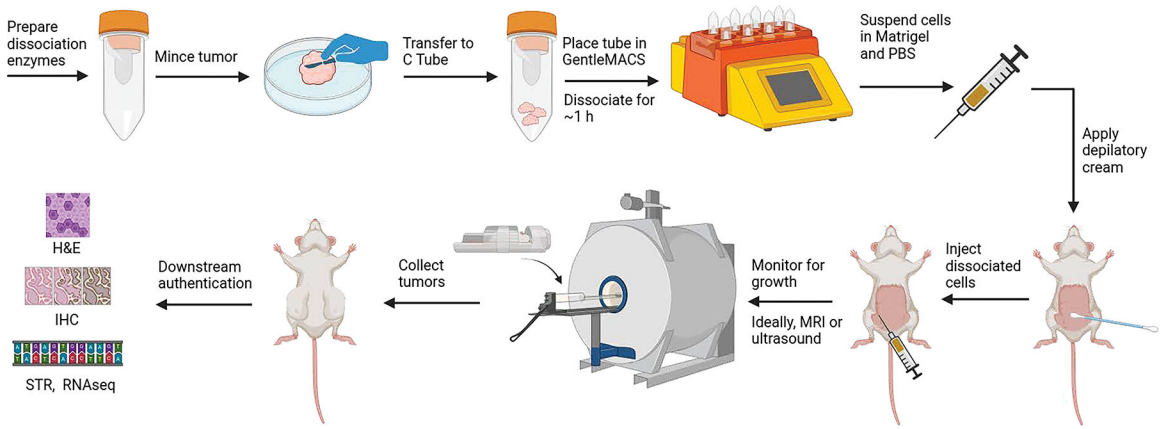

Figure 1: Overview of the protocol.

Representation of tumor dissociation and injection workflow. Please click here to view a larger version of this figure.

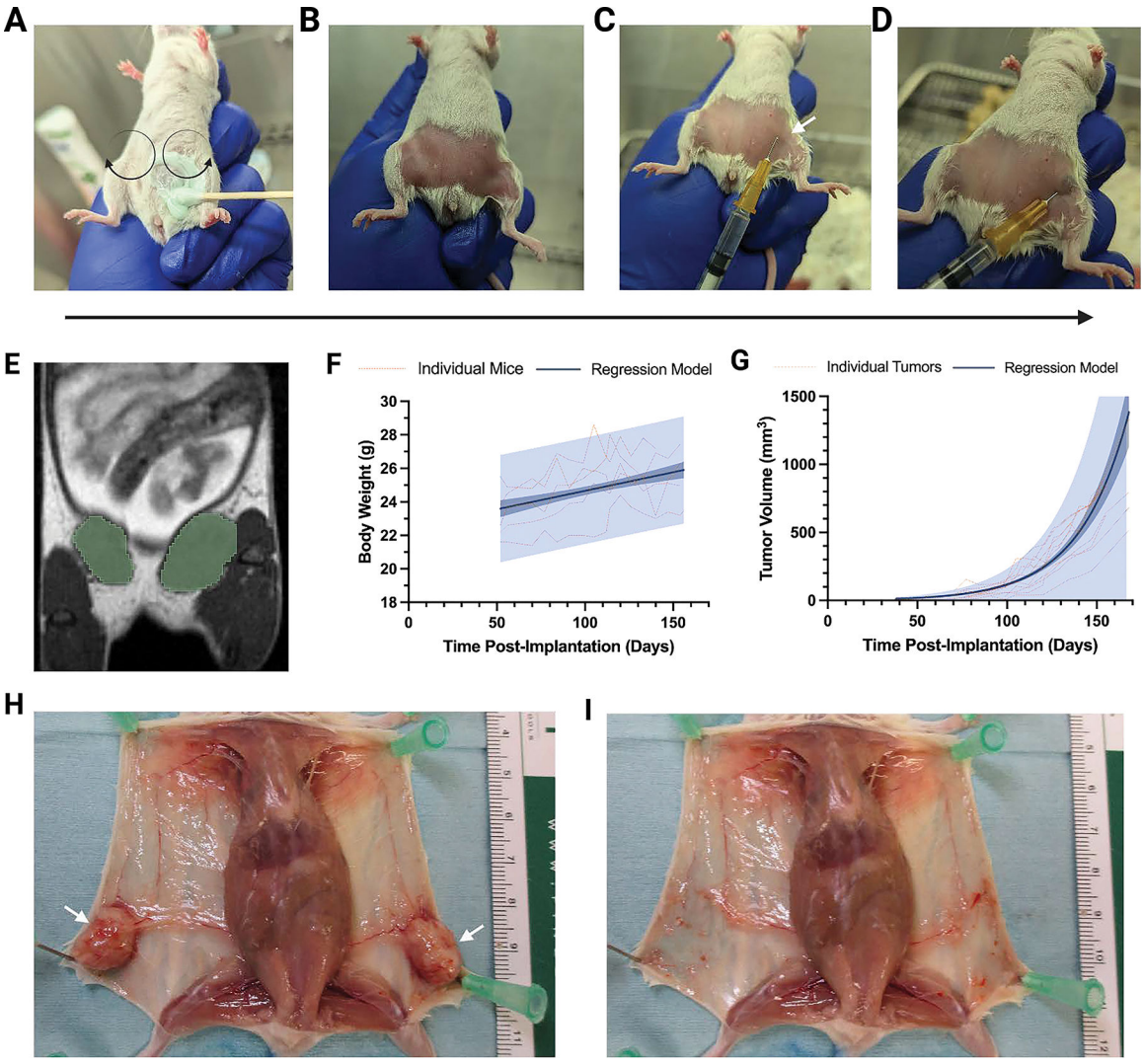

Figure 2: Preparation of mice, PDX injection, and monitoring of tumor progression.

(**A**) Mammary fat pads were thoroughly depilated. (**B**) Presentation of the injection site with clear visibility of the target injection areas. (**C**) Position of the syringe on the fat pad, typically 0.5–1 mm caudal to fat pad depending on needle length. The white arrow indicates the target area for the needle when inserting. (**D**) Depiction of dissociated cell injection into the left fourth inguinal nipple mammary fat pad. The needle should be held at an approximately 45-degree angle as shown for injection. (**E**) Representative MRI image of bilaterally engrafted tumors at injection site. Tumors are highlighted in green. (**F**) Representative progression of body weights in grams following tumor cell injection (n = 5). The dark blue line represents simple linear regression, which is significantly non-zero ($p < 0.0001$); mice gained, on average, 22 mg·day^{-1}. Dark blue shading is a 95% confidence interval, light blue shading is a 95% prediction interval, and orange lines are longitudinal body weight measurements. (**G**) Representative progression of individual tumor volumes in mm^3 following tumor cell injection (n = 10). The dark blue line represents exponential regression; tumor volume doubling time was 19.08 days. Dark blue shading is a 95% confidence interval, light blue shading is a 95% prediction interval, and orange lines are

longitudinal tumor volumes. (**H**) Successful bilateral engraftment of PDX cells into the inguinal mammary fat pads. Note that vascularization can be seen supplying each tumor. The white arrows identify the tumors. (**I**) The inguinal mammary fat pad area following the excision of tumors. (**H,I**) Units on the ruler are in cm. Please click here to view a larger version of this figure.

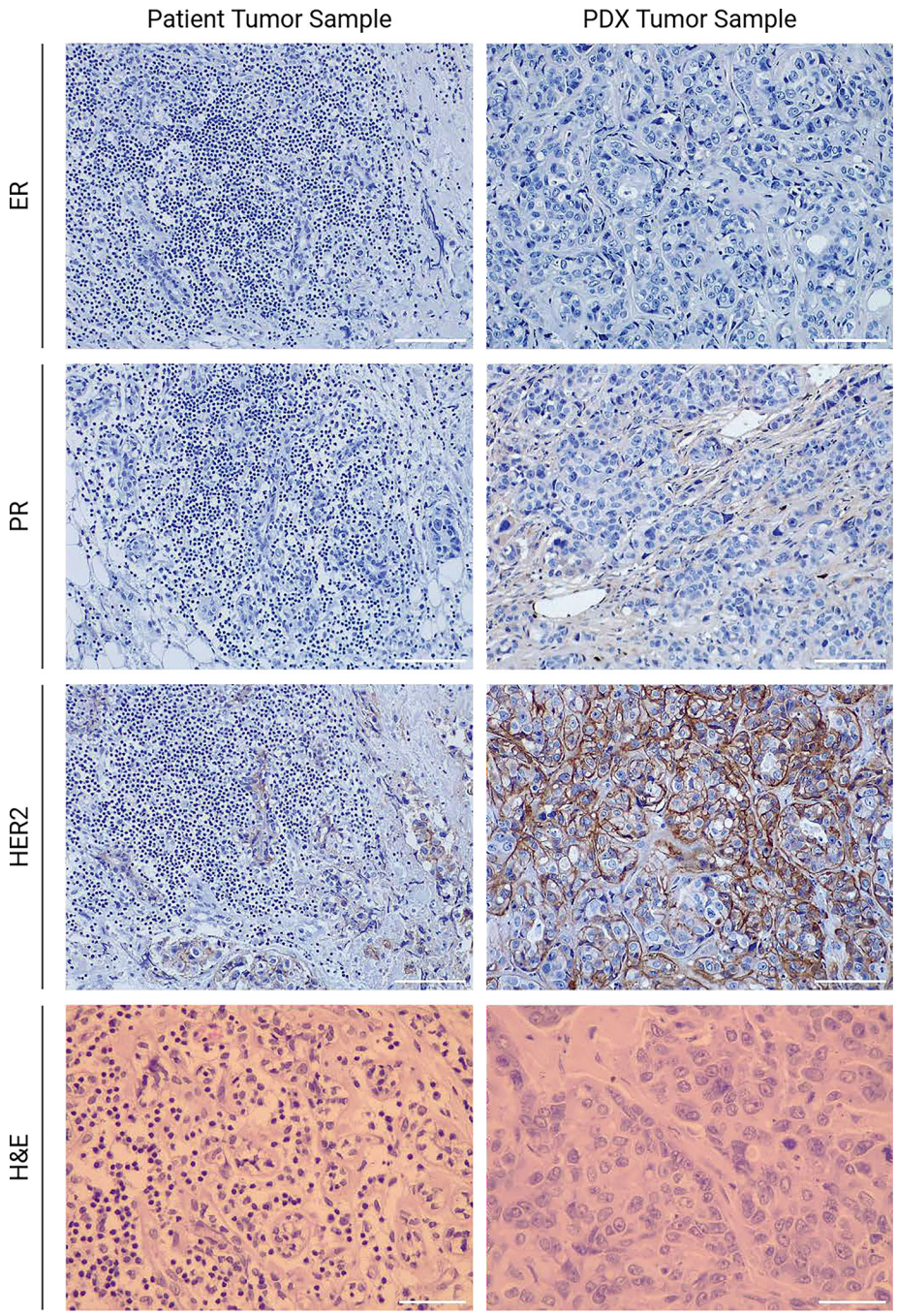

Figure 3: IHC receptor and H&E staining. (Left column)
IHC staining of ER, PR, and HER2 receptors and H&E staining in the patient tumor. ER and PR stains show no evident positive staining, as expected. HER2 stains display positivity for HER2 (brown). (**Right column**) IHC staining of ER, PR, and HER2 receptors and H&E staining in the passaged PDX sample. Receptor staining closely resembles that seen in the patient sample, although HER2 shows greater expression after passaging. Scale bar: 50 μm; magnification: 20x. Please click here to view a larger version of this figure.

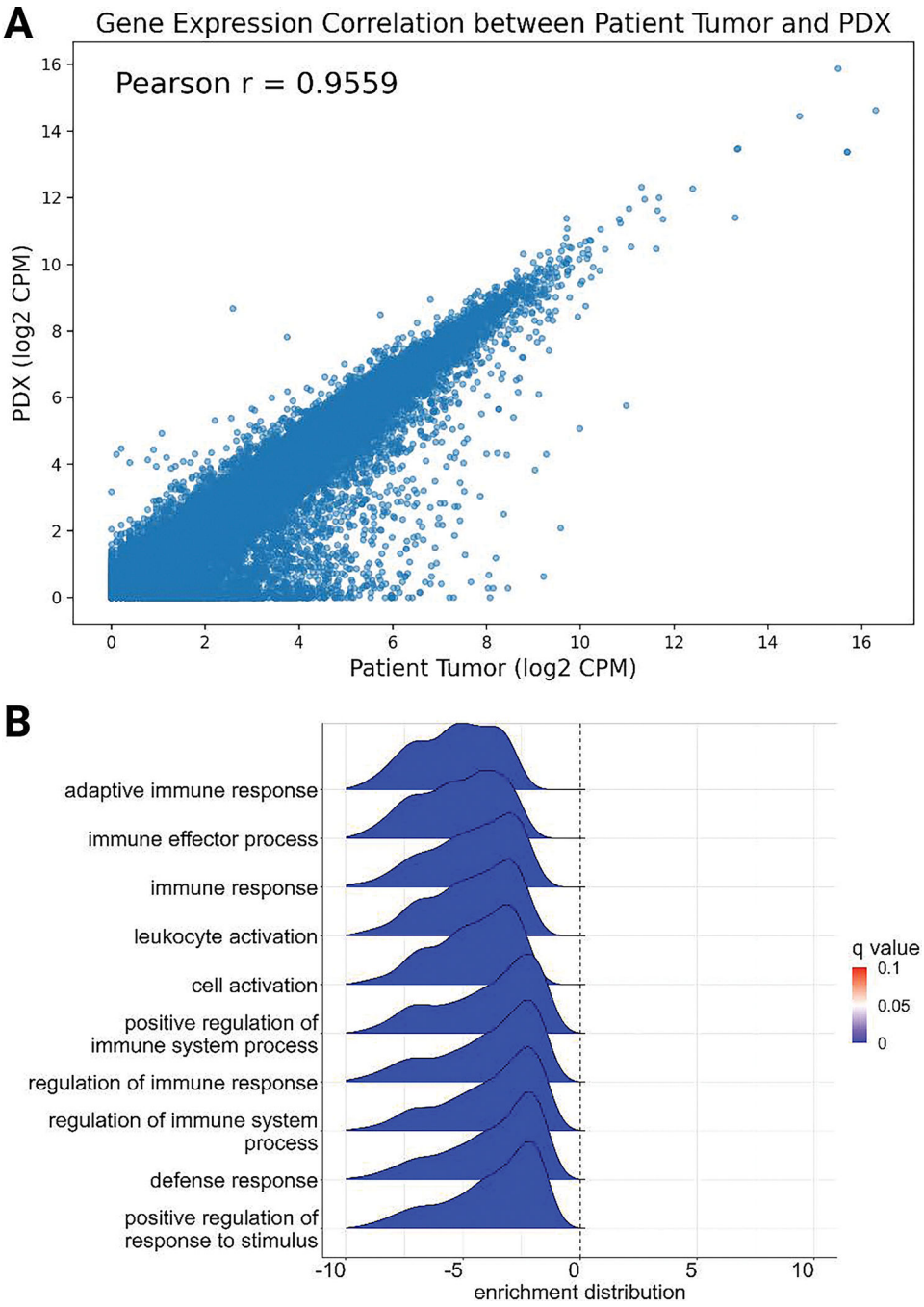

Figure 4: RNA-sequencing correlation and gene set enrichment.

(**A**) Scatter plot visualizing the log2 normalized counts per million (CPM) for all genes from the patient tumor (x-axis) and PDX (y-axis). A strong positive correlation was found, with a Pearson r value of 0.9559. (**B**) Ridge plots for the top 10 enriched gene ontology biological process gene sets when comparing PDX *vs.* patient tumor. Curves depict the enrichment score distribution for each gene set; color represents the FDR q-value for each gene set.

Please click here to view a larger version of this figure.

Table 1:

Short tandem repeat (STR) authentication.

	D5S818	D13S317	D7S820	VWA	TH01	AM	TPOX	CSF1PO	D3S1358	D21S11	D18S51	Penta_E	Penta_D	D8S1179	FGA
Patient	12	8	8	17	9	X	8		15	29	16	12	14	10	21
tumor	13	8	9	17	9.3	X	10		16	31.2	19	13	14	14	25
PDX	13	8	8	17	9	X	10		15	29	16	12	14	10	21
tumor	14	8	9	17	9.3	X	10		15	29	19	13	14	14	25

Table of Materials

Name of Material/ Equipment	Company	Catalog Number	Comments/ Description
1 mL tuberculin syringe	BD	305945	sterile
1X phosphate buffered saline, pH 7.4	Gibco	10010023	sterile
2.0 mL round-bottom microcentrifuge tube	Eppendorf	0030123620	sterile
26 gauge needle, ½ in.	BD	305111	sterile
5.0 mL microtube	Eppendorf	0030119401	sterile
8+ week old NSG (NOD.Cg-Prkdcscid Il2rgtm1Wjl/SzJ) mice	The Jackson Laboratory	#005557	
Alcohol prep pads	Fisher Scientific	22–363-750	sterile
Basement membrane extract (Matrigel)	Cultrex	3632–005-02	
Cotton-tipped applicators, 6 in.	Fisher Scientific	22–029-553	sterile
Curved Forceps with Medium Non-serrated Tips, 152 mm	Electron Microscopy Sciences	50–365-845	sterile
Depilatory cream	Nair		
gentleMACS C Tubes	Miltenyi Biotec	130–093-237	
gentleMACS Octo dissociator with heaters	Miltenyi Biotec	130–096-427	
No. 10 scalpel blades	Fisher Scientific	12–000-162	sterile
Non-woven gauze sponges, 4x4 inch	Fisher Scientific	22–028-558	sterile
RPMI 1640 1x + L-Glutamine	Gibco	11875093	sterile
Tumor dissociation kit, human	Miltenyi Biotec	130–095-929	